Appl Nanosci (2021) 11:2153–2165
DOI 10.1007/s13204-015-0484-9

ORIGINAL ARTICLE

One-step synthesized calcium phosphate-based material for the removal of alizarin S dye from aqueous solutions: isothermal, kinetics, and thermodynamics studies

Abideen Idowu Adeogun[1,2] · **Ramesh Balakrishnan Babu**[2]

Received: 30 June 2015 / Accepted: 15 July 2015 / Published online: 28 July 2015

Abstract Calcium phosphate hydroxyapatite (Ca-Hap) synthesized from $CaCO_3$ and H_3PO_5, it was characterized by scanning electron microscopy, Fourier transform infrared, and X-ray diffraction. The Ca-Hap was used for the removal of Alizarin Red S dye from its aqueous solution. The kinetics, equilibrium, and thermodynamic of the adsorption of the dye onto the Ca-Hap were investigated. The effects of contact time, initial dye concentration, pH as well as temperature on adsorption capacity of Ca-Hap were studied. Experimental data were analyzed using six model equations: Langmuir, Freudlinch, Redlich–Peterson, Temkin, Dubinin–Radushkevich, and Sips isotherms and it was found that the data fitted well with Sips and Dubinin–Radushkevich isotherm models. Pseudo-first-order, pseudo-second-order, Elovic, and Avrami kinetic models were used to test the experimental data in order to elucidate the kinetic adsorption process and it was found that pseudo-second-order model best fit the data. The calculated thermodynamics parameters ($\Delta G°$, $\Delta H°$ and $\Delta S°$) indicated that the process is spontaneous and endothermic in nature.

Keywords Calcium phosphate · Alizarin Red S · Adsorption · Kinetics · Thermodynamics · Equilibrium

✉ Abideen Idowu Adeogun
abuaisha2k3@yahoo.com

[1] Department of Chemistry, Federal University of Agriculture, Abeokuta, Nigeria

[2] Electrochemical Pollution Control Division, CSIR- Central Electrochemical Research Institute, Karaikudi 630006, India

Introduction

Environmental contaminations by toxic wastes pose a serious problem worldwide due to their incremental accumulation in the food chain and continued persistence in the ecosystem. The residual dyes from different sources such as: textile, paper and pulp, dye and dye intermediates, pharmaceutical, tannery, and kraft bleaching industries are considered as organic colored pollutants (Rajgopalan 1995; Routh 1998; Kolpin et al. 1999; Ali and Sreekrishnan 2001). These industries utilize large quantities of a number of dyes which residues lead to large amount of colored wastewaters, toxic and even carcinogenic, posing serious hazard to aquatic living organisms. Most dyes used in industries are stable to light, heat, and oxidation, they are not biologically degradable and are also resistant to aerobic digestion and even when they does, they produce toxic and hazardous products (Sun and Yang 2003; Shawabkeh and Tutunji 2003). Alizarin Red S (ARS) an anthraquinone dye is available as sodium salt of 1,2-dihydroxy-9,10-anthraquinonesulfonic acid (Fig. 1), it is referred to as Mordant Red 3, C.I. No. 58005. Alizarin a natural dye obtained from madder (*Rubia tinctorum*, L. Rubiaceae) by sulphonation, is a water-soluble, widely used anthraquinone dye in textile and as a stain in clinical study of synovial fluid to assess basic calcium phosphate crystals (Zucca et al. 2008). ARS is a durable pollutant when released to aquatic ecosystems. It cannot be completely degraded by general physicochemical and biological processes because of the complex structures of the aromatic rings that afford high physicochemical, thermal, and optical stability (Carneiro et al. 2005; Panizza et al. 2001). Therefore, most treatments for such dye-laden effluents are largely inadequate; however, removal of this dye from industrial wastewaters is a crucial process, from both economic and environmental points of view (Panizza et al. 2001).

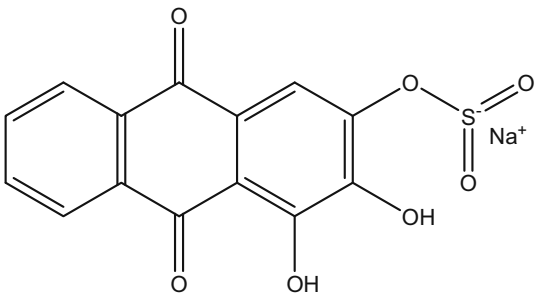

Fig. 1 Structure of Alizarin Red S (ARS)

Convectional technologies, such as ion exchange, chemical precipitation, oxidation reduction, filtration, electrochemical techniques, and other sophisticated separation processes using membranes, are often ineffective and/or expensive. Furthermore, most of these techniques are based on physical displacement or chemical replacement, generating yet another problem in the form of toxic sludge, the disposal of which adds further burden on the techno-economic feasibility of the treatment process. Recently, calcium phosphates, and particularly calcium hydroxyapatite (Ca-HA), attracted much interest because of their high potential application for the remediation of toxic materials in liquid wastes coupled with their biocompatibility and low cost. For example, hydroxyapatites have been employed as inorganic cation exchangers, for removal of lead, cadmium, and nickel ion from aqueous solution (Suzuki et al. 1984; Miyake et al. 1990; Ma et al. 1994; Nzihou and Sharrock 2010; Nzihou and Sharrock 2010; Minh et al. 2012, 2014; Mobasherpour et al. 2012). Nano crystalline hydroxyapatite also served as adsorbents for the adsorption and separation of biomolecules (Wei et al. 2009; Takagi et al. 2004) and removal of dye molecules from aqueous solution (El Boujaady et al. 2014).

In this study, a one-step approach was adopted for the preparation of calcium phosphate (Ca-P)-based materials starting from calcium carbonate and orthophosphoric acid for the removal of alizarin dye from aqueous solution. The material was characterized by scanning electron microscopy (SEM), Fourier transform infrared (FTIR), and X-ray diffraction (XRD). A series of adsorption experiments on the removal of the dye from aqueous solution were investigated in a batch system. The effect of solution pH, initial contaminants concentrations, and contact time were also studied.

Materials and methods

Synthesis of calcium phosphate

All the chemicals used in this study were analytical grade which includes $CaCO_3$, H_3PO_5, NH_4OH, HCl, NaOH, and ARS. Hydroxyapatite Calcium Phosphate was synthesized in a three necked flask. Slurry of 150 mL of 0.1 M $CaCO_3$ in was made quantitatively in the flask and stirred to make a uniform disperse. Then, 150 mL of 0.6 M H_3PO_5 was added slowly for 4 h with constant stirring while the temperature was maintained at 80 °C. The pH was maintained at 9.5 with 25 % NH_4OH. The stirring was continued for 24 h after which the mixture is allowed to age for another 24 h after, when it was filtered off and dry at 106 °C.

Analytical procedure

The dried material was characterized by different physicochemical techniques. XRD data were collected using a PAN Analytical X'Pert PRO X-ray diffractometer with Cu Kα radiation ($\lambda = 1.5418$ Å). FTIR spectra were recorded from 400 to 4000 cm^{-1} in TENSOR 27 spectrometer (Bruker, Germany) using KBr pellet technique. Surface morphology of the material was analysed using SEM [VEGA3 TESCAN]. The concentrations of the dye in the solutions were estimated using spectrophotometer (UV–VIS–NIR VARIAN 500 Scan CARY). Non-linear regression analysis method using a program written on Micro Math Scientist software (Salt Lake City, Utah) was used to obtain the least square fit for all the models.

Equilibrium studies

The effects of adsorbent dosage, initial dye concentration, pH, and temperature on the adsorption removal of ARS were studied. Sample solutions were withdrawn at intervals to determine the residual dye concentration by using UV–VIS–NIR spectrophotometer. The amount of dye removed at equilibrium, Q_e (mg g^{-1}), was calculated using Eq. (1) below:

$$Q_e = \frac{(C_o - C_e)V}{W}, \quad (1)$$

where C_o (mg L^{-1}) is the initial concentration and C_e (mg L^{-1}) is the concentration of the dye at equilibrium in the liquid-phase. V is the volume of the solution (L) while W is the mass of the adsorbent. The percentage dye removal as color removal is also estimated as

$$\% \text{ Color removal} = \frac{(\text{Abs}_o - \text{Abs}_e) \times 100}{\text{Abs}_0}, \quad (2)$$

where Abs_o, is the blank absorbance and Abs_e is the absorbance at equilibrium.

Effect of adsorbent dosage

The study of effect of adsorbent dosages for removal of ARS from aqueous solution was carried out at different adsorbent doses ranging between 0.1 and 1.0 g using

50.0 mg L^{-1} of the dye solution. The Erlenmeyer flasks containing the dye solutions of the same initial concentration but different adsorbent masses were placed on orbital shaker at 200 rpm. After some time, the samples were filtered off and the dye solution was analyzed for the residual dye content using UV visible spectrophotometer.

Effects of initial dye concentration and contact time

The effects of initial dye concentration and contact time on adsorption were investigated with 100 mL dye solution of initial concentrations between 25 and 150 mg L^{-1} in series of Erlenmeyer flasks with fixed amount of adsorbent (0.1 g) on orbital shaker at 200 rpm. Samples were withdrawn and analyzed for the residual dye from the aqueous at preset time intervals.

Effect of pH on adsorption process

pH plays an important role on adsorption process of dye by influencing the chemistry of the adsorbent, dye molecule and that of adsorption process in the solution. To investigate the effect pH, on the removal of ARS, a series of experiments were carried out on solutions with initial pH varied between 3 and 11. The pH was adjusted with 0.1 M NaOH or 0.1 M HCl and measured using pH meter. The concentrations of the solutions, adsorbent dosage, and temperature were held constant at 50 mg L^{-1}, 0.1 g and 30 °C, respectively.

Adsorption isotherms

The equilibrium data from this study were described with the six adsorption isotherm models. These are models by Langmuir (1918), Freudlinch (1906), Tempkin and Pyzhev (1940), Dubinin and Radushkevich (1947), Sips (1948) and Redlich and Peterson (1959). The acceptability and suitability of the isotherm equation to the equilibrium data were based on the values of the correlation coefficients, R^2 estimated from linear regression of the least square fit statistic on Micro Math Scientist software.

Langmuir isotherms

The Langmuir isotherm equation is based on the following assumptions: (1) that the entire surface for the adsorption has the same activity for adsorption, (2) that there is no interaction between adsorbed molecules and (3) that all the adsorption occurs by the same mechanism and the extent of adsorption is less than one complete monomolecular layer on the surface. The Langmuir equation is given by Eq. (3) (Langmuir 1918):

$$Q_{eq} = \frac{Q_o b C_e}{1 + bC_e}, \tag{3}$$

where Q_o is the maximum amount of the dye molecule per unit weight of the coagulant to form a complete monolayer on the surface C_e (mg g^{-1}) is the concentration of the dye remaining in solution at equilibrium and b is equilibrium constant (L mg^{-1}). The shape of Langmuir Isotherm can be used to predict whether a process is favorable or unfavorable in a batch adsorption process. The essential features of the Langmuir isotherm can be expressed in terms of a dimensionless constant separation factor (R_L) that can be defined by the following relationship (Aniruldhan and Radhakrishnan 2008):

$$R_L = \frac{1}{1 + bC_0}, \tag{4}$$

where C_o is the initial concentration (mg L^{-1}) and b is the Langmuir equilibrium constant (L mg^{-1}). The value of separation parameter R_L provides important information about the nature of adsorption. The value of R_L indicated the type of Langmuir isotherm to be irreversible if $R_L = 0$, favorable when $0 < R_L < 1$, linear when $R_L = 1$ and unfavorable when $R_L > 1$. However, it can be explained apparently that when $b > 0$, sorption system is favorable (Aniruldhan and Radhakrishnan 2008).

Freundlich isotherm

The Freundlich isotherm is an empirical equation based on sorption on a heterogeneous surface. It is commonly presented as

$$Q_{eq} = K_F C_e^{1/n}, \tag{5}$$

where K_F and n are the Freundlich constants related to the adsorption capacity and intensity of the sorbent, respectively (Bello et al. 2008; Adeogun et al. 2012).

Redlich–Peterson isotherm

A three parameters Redlich–Peterson equation has been proposed to improve the fit by the Langmuir or Freundlich equation and is given by Eq. (6).

$$Q_{eq} = \frac{Q_o C_e}{1 + K_R C_e^{\beta}}, \tag{6}$$

where K_R and β are the Redlich–Peterson parameters, β lies between 0 and 1 and for $\beta = 1$, Eq. (6) converts to the Langmuir form.

Tempkin isotherm model

Temkin isotherm model was also used to fit the experimental data. Unlike the Langmuir and Freundlich equations, the Temkin isotherm takes into account the interaction between sorbent and adsorbent. It is based on the assumption that the free energy of sorption is a function of the surface coverage (Adeogun et al. 2012). The Tempkin isotherm is represented as in Eq. (7):

$$Q_e = \frac{RT}{b_T} \ln a_T C_e, \tag{7}$$

where C_e is concentration of dye in solution at equilibrium (mg L^{-1}), Q_e is the amount of dye molecule coagulated at equilibrium (mg g^{-1}), T is the temperature (K), and R is the ideal gas constant (8.314 J mol^{-1} K^{-1}) and 'a_T' and 'b_T', are constants relating to binding constant (L mg^{-1}) equilibrium corresponding to the maximum bonding energy and the heat of adsorption, respectively.

The Dubinin–Radushkevich isotherm

The Dubinin–Radushkevich model (Dubinin and Radushkevich 1947) was chosen to estimate the heterogeneity of the surface energies and also to determine the nature of adsorption processes as physical or chemical. The D–R sorption isotherm is more general than the Langmuir isotherm as its derivation is based on ideal assumptions such as equipotent of the sorption sites, absence of stoic hindrance between sorbed and incoming particles and surface homogeneity on microscopic level (Weber and Morris 1963; Malik 2004). D–R isotherm is represented by Eq. (8) below:

$$Q_e = Q_m e^{-\beta \varepsilon^2}, \tag{8}$$

where Q_m is the theoretical saturation capacity (mol g^{-1}), β is a constant related to the mean free energy of adsorption per mole of the adsorbate (mol^2 J^{-2}), and ε is the Polanyi potential given by the relation; $\varepsilon = \ln\left(1 + {}^1/_{C_e}\right)$. C_e is the equilibrium concentration of dye in solution (mg L^{-1}), R (J mol^{-1} K^{-1}) is the gas constant and T (K) is the absolute temperature. The constant β gives an idea about the mean free energy E (kJ mol^{-1}) of adsorption per molecule of the adsorbate when it is transferred to the surface of the solid from relationship (Malik 2004).

$$E = (2\beta)^{-0.5}. \tag{9}$$

If the magnitude of E is between 8 and 16 kJ mol^{-1}, the process is chemisorption, while for values of $E < 8$ kJ mol^{-1} suggests a physical process.

The Sips isotherm

The Sips isotherm model is a combined form of the Langmuir and Freundlich expressions deduced for predicting the heterogeneous adsorption systems and circumventing the limitation of the rising adsorbate concentration associated with the Freundlich isotherm model (Sips 1948). At high adsorbate concentration, it predicts monolayer adsorption characteristics of Langmuir isotherm, while at low adsorbate concentration, it reduces to Freundlich isotherm. The Sips model is expressed as Eq. (10) below:

$$Q_{eq} = \frac{Q_o (k_s C_e)^{m_s}}{1 + (k_s C_e)^{m_s}}, \tag{10}$$

where k_s is the Sips isotherm model constant and m_s is the Sips isotherm model exponent.

Adsorption kinetics studies

The procedures for the kinetics studies were basically identical to those of equilibrium tests. The aqueous solutions of known dye concentration with a predetermined amount of adsorbent were placed in Erlenmeyer flasks in an orbital shaker, samples were taken at preset time intervals, and the concentrations of the dye were similarly determined. The amount of dye removed at time t, Q_t (mg g^{-1}), was calculated using Eq. (11):

$$Q_t = \frac{(C_o - C_t)V}{W}, \tag{11}$$

where C_o (mg L^{-1}) is the initial concentration and C_t (mg L^{-1}) is the concentration of the dye at time t in the liquid-phase. V is the volume of the solution (L), and W is the mass of adsorbent. In order to investigate the mechanisms of the adsorption process, pseudo-first order, pseudo-second-order, Avrami, and Elovich models, respectively, were applied to describe the kinetics of adsorption of ARS to calcium phosphate. A model is adjudged best-fit and selected based on statistical parameters.

The pseudo-first order kinetics model

A simple kinetics analysis of the process under the pseudo-first order assumption is given by Eq. (12) below (Lin and Brusick 1992; Kundu and Gupta 2006):

$$\frac{dQ}{dt} = k_1 (Q_e - Q_t), \tag{12}$$

where Q_e and Q_t are the dye concentrations (mg g^{-1}) at equilibrium and at time t (min), respectively, and k_1 the adsorption rate constant (min^{-1}), and t is the contact time (min). The integration of Eq. (16) with initial

concentrations, $Q_t = 0$ at $t = 0$, and $Q_t = Q_t$ at $t = t$, yields Eq. (13) below:

$$\ln(Q_e - Q_t) = \ln Q_e - k_1 t. \quad (13)$$

Upon rearrangement, Eq. (13) becomes:

$$Q_t = Q_e(1 - e^{-k_1 t}). \quad (14)$$

The values of Q_e and k_1 were calculated from the least square fit of Q_t versus t at different dye concentrations.

The pseudo-second order kinetics model

A pseudo-second order kinetics model is based on equilibrium adsorption (Bello et al. 2008; Kundu and Gupta 2006) and it is expressed as shown Eq. (15) below:

$$t/Q_t = 1/k_2 Q_e^2 + (1/Q_t)t. \quad (15)$$

The expression above can also be rearranged to give Eq. (16) below:

$$Q_t = \frac{k_2 Q_e^2 t}{1 + k_2 Q_e t}, \quad (16)$$

where k_2 (g mg^{-1} min^{-1}) is the rates constant of pseudo-second order adsorption, The values of Q_e and k_2 were calculated from the least square fit of Q_t versus t at different dye concentrations.

Elovich model

Elovich model is a kinetic equation describing a chemisorption process (Chien and Clayton 1980), it describes the rate of adsorption which decreases exponentially with an increase in the adsorbed. It is generally expressed as shown by Eq. (17) (Chien and Clayton 1980):

$$Q_t = 1/\beta \ln(\alpha\beta * t), \quad (17)$$

where α is the initial adsorption rate (mg g^{-1} min^{-1}), β is the desorption constant (g mg^{-1}). The value of reciprocal of β reflects the number of sites available for adsorption, whereas the value of adsorbed quantity when t is equal to zero is given by $1/\beta \ln(\alpha\beta)$.

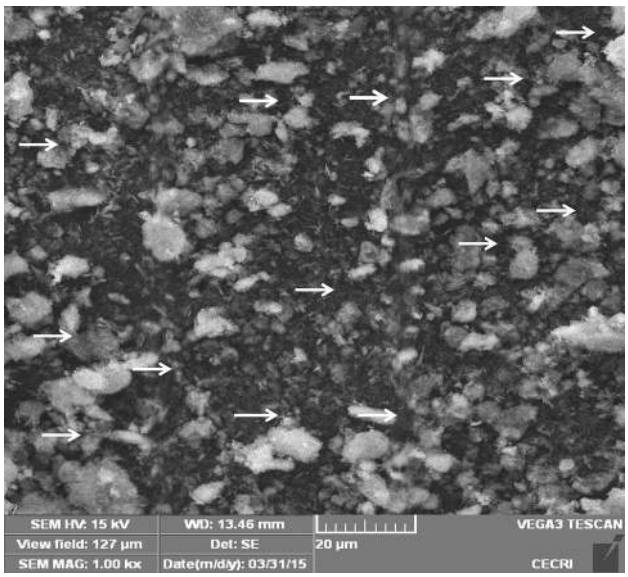

Fig. 3 Scanning electron micrograph of the synthesized powders

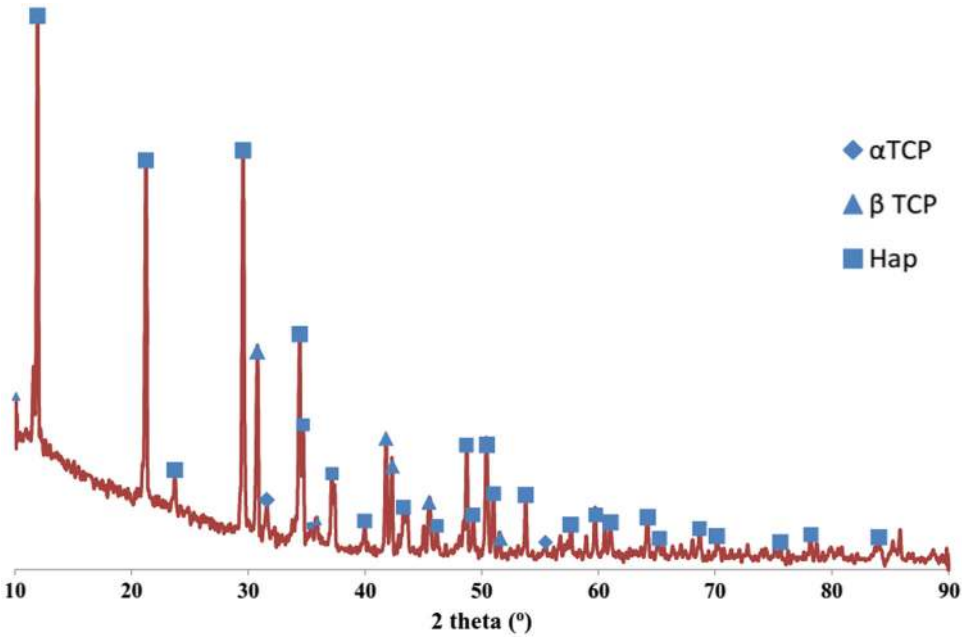

Fig. 2 XRD patterns of the synthesized powders

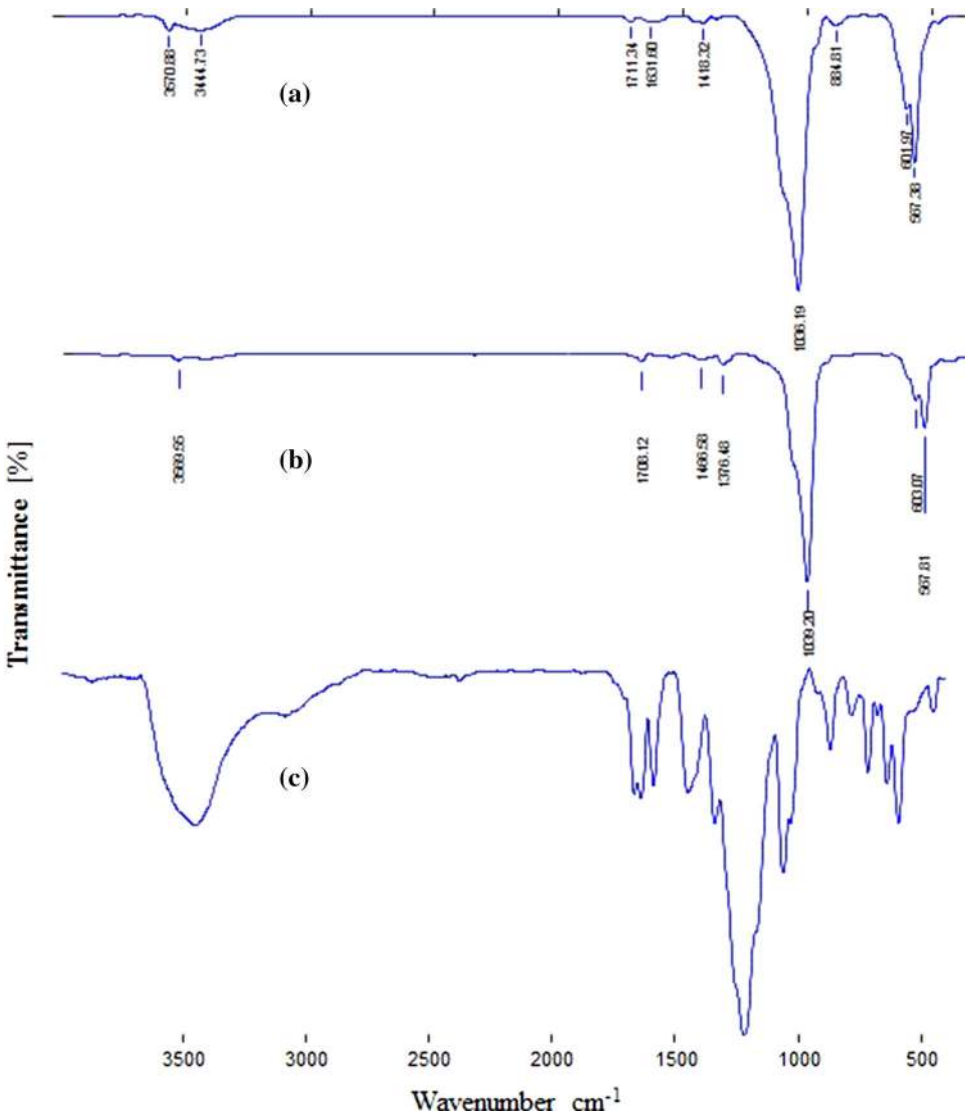

Fig. 4 FTIR spectrum: **a** Ca-Hap before adsorption, **b** after adsorption, and **c** Alizarin S dye

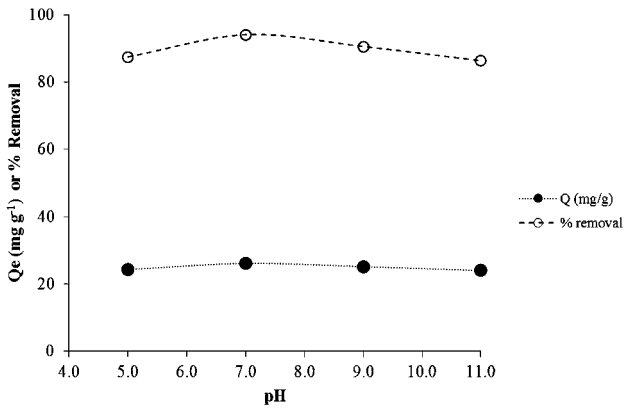

Fig. 5 Effect of pH on the adsorption process

Statistical test for the kinetics data

The acceptability and hence the best fit of the kinetic data were based on the square of the correlation coefficients R^2 and the percentage error function which measures the differences (% SSE) in the amount of the dye concentration coagulated at equilibrium predicted by the models, (Q_{cal}) and the actual, (i.e., Q_{exp}) measured experimentally. The validity of each model was determined by the sum of error squares (SSE, %) given by:

$$\%\ SSE = \sqrt{\frac{\left(\left(Q_{(exp)} - Q_{(cal)}\right)/Q_{exp}\right)^2}{N-1}} \times 100. \quad (18)$$

N is the number of data points. The higher is the value of R^2 and the lower the value of SSE; the better fitted the data.

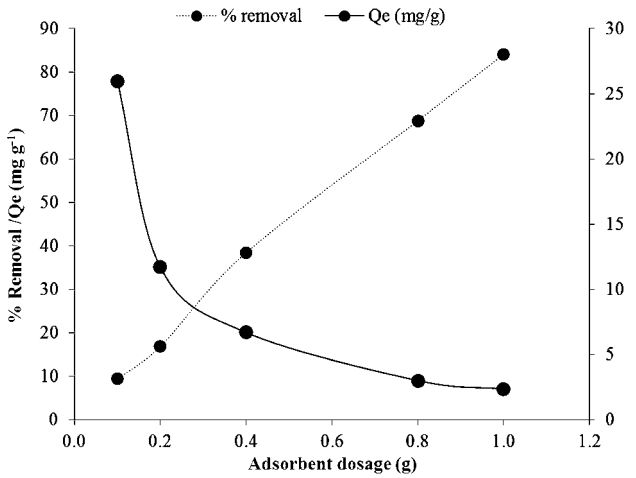

Fig. 6 Effect Adsorbent dosage on the adsorption process

Intra-particulate diffusion model

Due to the fact that the diffusion mechanism cannot be obtained from the kinetics model, the intraparticlate diffusion model (Wu et al. 2009) was also tested. The initial rate of the intraparticle diffusion is given by the following expression:

$$Q_t = K_{\mathrm{id}} t^{0.5} + C_i, \tag{19}$$

where K_{id} is the intraparticle diffusion rate constant (mg g^{-1} $min^{-0.5}$) and C_i is intercept and a measure of surface thickness.

Thermodynamics of adsorption process

The thermodynamics parameters i.e., $\Delta G°$, $\Delta H°$, and $\Delta S°$ were estimated using the following relation (Lyubchik et al. 2011):

$$\Delta G^\circ = -RT \ln K_{\mathrm{d}}, \tag{20}$$

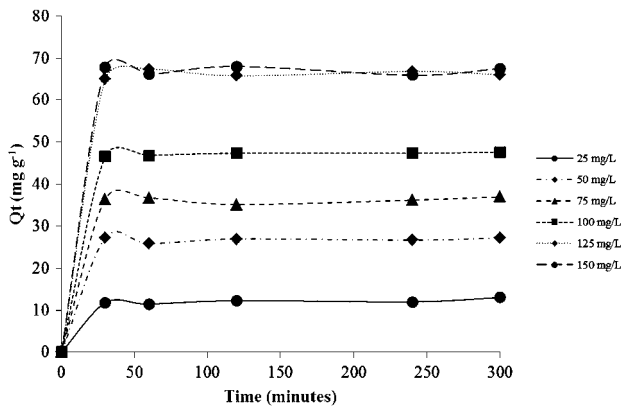

Fig. 7 Effect of initial dye concentration on the adsorption process

$$\ln K_{\mathrm{d}} = \frac{\Delta S^\circ}{R} - \frac{\Delta H^\circ}{RT}. \tag{21}$$

The equilibrium constant, K_{d}, is obtained from the value of Q_e/C_e at different temperature equilibrium studies. Van't Hoff plot of ln K_{d} against the reciprocal of temperature (1/T), should give a straight line with intercept as $\frac{\Delta S^\circ}{R}$ and slope as $\frac{\Delta H^\circ}{R}$.

Result and discussion

Synthesis and characterization of calcium phosphate

The XRD pattern for the synthesized Ca-Hap powder is shown in Fig. 2. All reflections can be accounted for using the reference spectra for HA, β-TCP, and α-TCP, with no other significant phases present. The major peaks in are from hydroxyapatite which contains sharp and strong peaks due to the high degree of crystallinity of the powder. The three highest peaks of appears at $2\theta = 11.79$, 21.08, and 29.42. The phase composition indicates that the majority of the material remains as HA, with the remainder composed of TCP phases. SEM micrograph of the synthesized calcium phosphate (Fig. 3) showed that the powder layer exhibited a porous microstructure with micropores which were relatively well separated and homogeneously distributed over the surface. The FTIR spectra of the synthesized Ca-Hap powder are shown in Fig. 4. Typical absorption bands at 884.81, 567.38, 601.97, and 1036.19 cm^{-1} related to the nodes of phosphate and the broad band at 3444.7 and 3670.8 cm^{-1} are assigned to the hydroxyl while those at 1711.34, 1631.60, and 1418.32 cm^{-1} can be attributed to the water molecule present in the powder. Upon the adsorption of the dye molecule, the spectra changed drastically as shown in (b) the band at 884.81 cm^{-1} disappeared, while others undergo a reduction in intensity and little shifts. It is worth noting that the OH^- is still retained although the intensity is reduced which may be as a result of H-bonding interactions with the dye molecule.

Batch equilibrium studies

Effect of pH on adsorption process

One of the major factors affecting the adsorption of a dye on an adsorbent is the pH of the adsorbate solution (Royer et al. 2009). It affects the chemistry of both the adsorbent and the dye in the solution. The percentages color removal and adsorption capacity variation with pH is shown in Fig. 5. At pH lower than 5, the adsorbent (Ca-P) dissolved in the solution and as such limited the study to pH 5 and above. The color removal efficiency and adsorption capacity are optimum at the at pH range of 7.0 and 8.0 with

Table 1 Properties of Alizarin Red S (ARS)

Properties	
Chemical name	1,2-Dihydroxy-9,10-anthracenedione
Common name	Alizarin Red S
Generic name	Mordant Red 3
CAS number	72-48-0
Color index number	58005
Maximum wavelength	412 nm
Empirical formula	$C_{14}H_8O_4$
Molecular weight	240.21 g mol^{-1}

about 95 % color removal efficiency. This observation is due to the fact that at higher pH, the OH^- predominates the surface of the adsorbent and the interaction is solely between the negatively charged dye molecules and Ca^{2+} presents at the adsorbent surface (Mobasherpour et al. 2012).

Effect of adsorbent dosage

The effect of adsorbent dosage on the efficiency of color removal by Calcium Phosphate during the adsorption

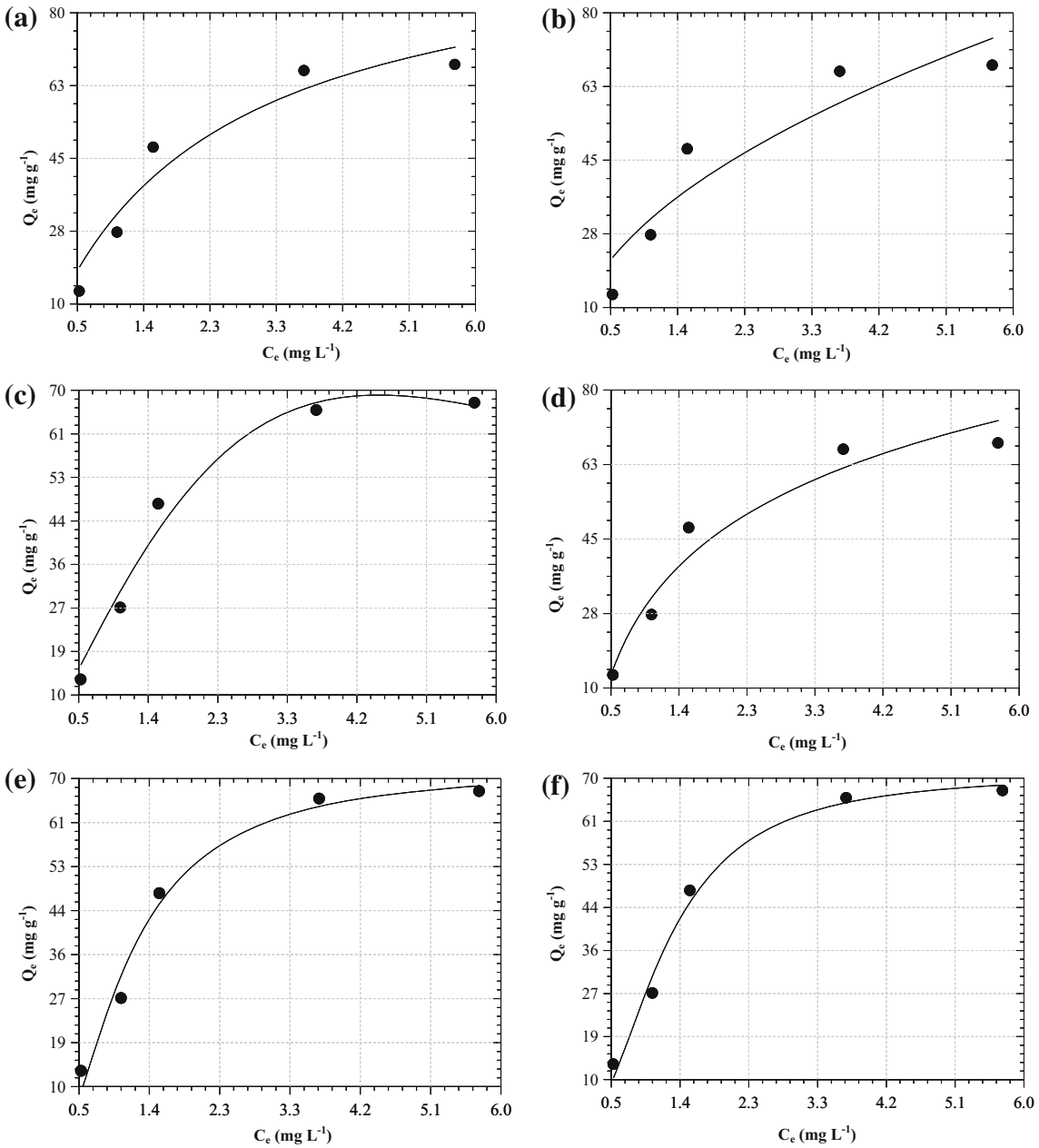

Fig. 8 Least square plots of the **a** Langmuir, **b** Freundlich, **c** Redlich–Peterson, **d** Temkin, **e** Dubinin–Radushkevich, and **f** Sips isotherm for the adsorption of ARS on Ca-P

process was investigated using various amount of the CaP. Figure 6 shows the plot of adsorbent dosage versus the percentage color removal and Q_e (mg g^{-1}) during the adsorption process. From the figure, it is glaring that as the adsorbent dosage is increased the percentage color removal increases from 9.3 to about 84.0 %, this is attributed to increase in the adsorption sites as the adsorbent dosage increases. On the contrary, the adsorption capacity decrease with increase dosage is mainly due to the increase of free adsorption sites as the dosage increases.

Effect of initial dye concentrations and contact time

The effect of initial dye concentration on the adsorption removal of ARS is shown in Fig. 7 for dye concentrations increasing from 25 to 150 mg L^{-1}. The process showed rapid removal in the first 30 min for all the concentrations studied. The efficiency of the process increases from 11.72 to 67.76 mg g^{-1} as the initial concentration increase from 25 to 150 mg L^{-1}. As there is no significant difference in the amount adsorbed after 60 min of the process, a steady-state approximation was assumed and a quasi-equilibrium situation was reached. The adsorption curves were single, smooth, and continuous, leading to saturation. This is an indication of possible monolayer coverage on the surface of the adsorbent. Also at low concentration of the dye molecule, there is a significant increase in dye adsorption capacity as a result of considerable amount of active site on adsorbent's surface was occupied by small amount of dye, making the adsorption capacities to become slower due to the saturation of active sites and hence longer time for equilibrium (Table 1).

Adsorption study

Adsorption isotherms

The adsorption data obtained at different initial dye concentrations were fitted into six different isotherm models as shown in Fig. 8. Table 2 showed the values of maximum adsorption capacities (Q_m), correlation coefficients (R^2), and other constant parameters for the six isotherm models equations for the adsorption process at 30 °C. For the Langmuir isotherm, the Q_m value of 100.36 mg g^{-1} was obtained and the value of R^2 of 0.988 shows good fitting of this isotherm to the experimental data (Table 5). The separation factor (R_L), an important parameter of the Langmuir isotherm was 0.035 (average of six concentrations) indicate favorable adsorption of the ARS onto Ca-P. The decrease in R_L with an increase in the initial concentration indicates that the adsorption is more favorable at high concentrations (figure not shown). Freundlich isotherm's constant, K_F is 30.32 mg g^{-1} (mg L^{-1})$^{-1/n}$ ($R^2 = 0.976$)

Table 2 Isotherm values for the adsorption of ARS on Ca-P

Langmuir		Freudlinch		Redlich–Peterson		Tempkin		Dubinin–Radushkevich		Sips	
Q_{max} (mg g^{-1})	100.36	K_F (mg g^{-1} (mg L^{-1})$^{-1/n}$)	30.32	Q_0 (L mg^{-1})g	106.56	b_T	102.76	Q (mg g^{-1})	71.92	Q_{max} (mg g^{-1})	48.49
b (L mg^{-1})	0.44	n	1.96	K_R (L g^{-1})	2.50	a_T (L g^{-1})	3.41	β (mol J^{-1})^2	2.89×10^{-7}	K_s (L mg^{-1})^{ns}	0.68
R_L	0.035			β	0.62			E (kJ mol^{-1})	1.32	m_s	2.18
R^2	0.988	R^2	0.976	R^2	0.980	R^2	0.991	R^2	0.997	R^2	0.998

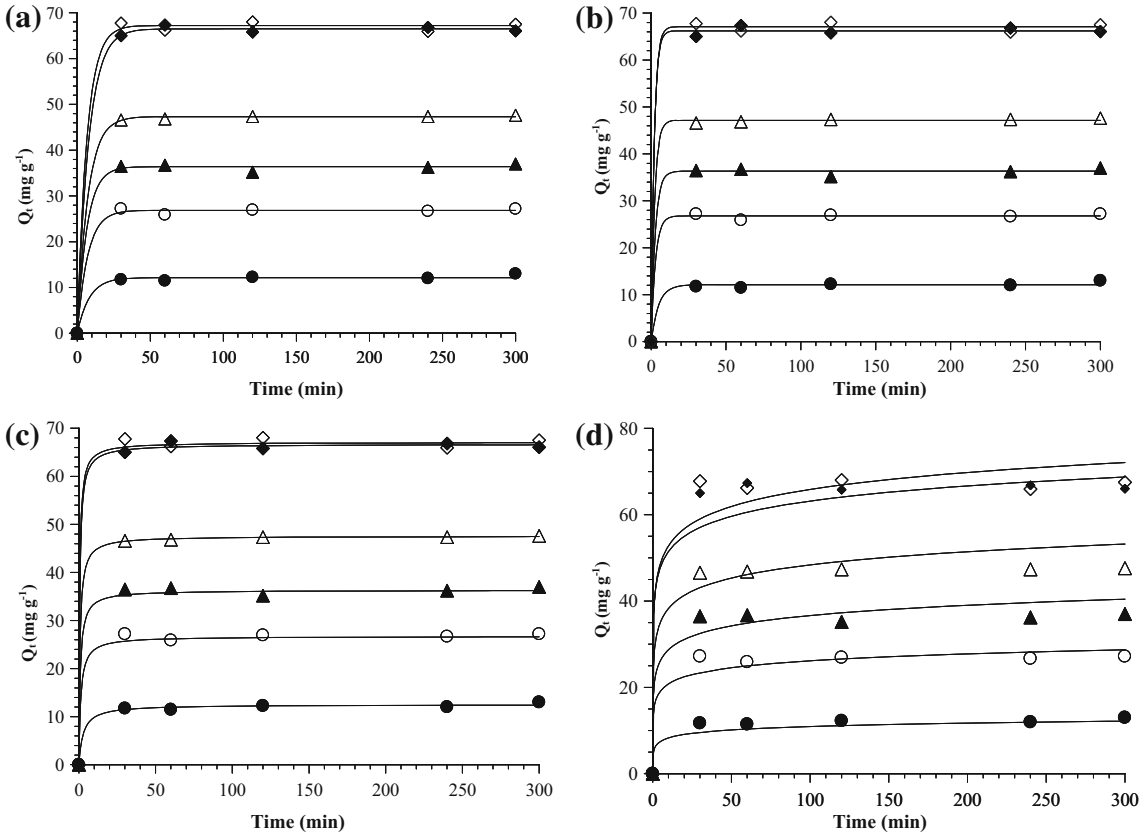

Fig. 9 Least square plots of **a** pseudo-first-order, **b** pseudo-second-order, **c** Avramin, and **d** Elovich kinetic models for the adsorption of ARS on Ca-P

Table 3 Kinetic parameters for the adsorption of ARS on Ca-P

		25 mg L^{-1}	50 mg L^{-1}	75 mg L^{-1}	100 mg L^{-1}	125 mg L^{-1}	150 mg L^{-1}
	$Q_{e\ exp}$ (mg g^{-1})	13.01	27.18	36.98	47.60	66.04	67.50
First order	$Q_{e\ cal}$ (mg g^{-1})	12.15	26.85	36.38	47.29	66.49	67.22
	k_1 (min^{-1})	0.12	0.14	0.15	0.14	0.13	0.15
	R^2	0.998	0.999	0.999	0.999	0.999	0.999
	% SSE	2.72	0.49	0.66	0.27	0.28	0.17
Avramin	$Q_{e\ cal}$ (mg g^{-1})	12.09	26.77	36.30	47.13	66.20	67.08
	k_{av} (min^{-1})	0.64	0.76	0.39	0.48	0.81	0.64
	n_{av}	0.32	0.47	0.94	0.89	0.61	0.75
	R^2	0.991	0.998	0.998	0.999	0.999	0.999
	% SSE	2.90	0.61	0.75	0.40	0.10	0.25
Second order	$Q_{e\ cal}$ (mg g^{-1})	12.50	26.69	36.31	47.56	66.67	67.10
	$k_{2\times10}^{-2}$ (g mg^{-1} min^{-1})	2.95	3.22	3.22	3.00	2.77	3.22
	R^2	0.999	0.999	0.999	0.999	0.999	0.999
	% SSE	1.59	0.73	0.73	0.03	0.39	0.24
Elovich	β (g mg^{-1})	0.77	0.40	0.28	0.23	0.18	0.16
	α (mg (g $min)^{-1}$)	149.89	1743.08	1461.11	2987.73	11,960.69	5762.33
	$Q_{t=0}$ (mg g^{-1})	6.18	16.26	21.30	28.81	42.99	41.91
	R^2	0.995	0.991	0.990	0.991	0.980	0.989

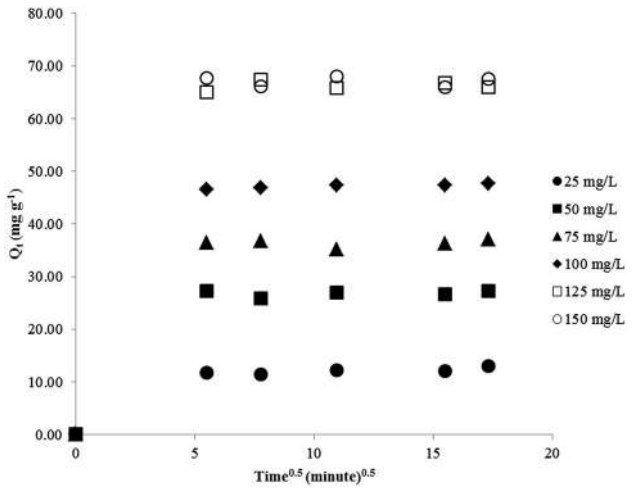

Fig. 10 Intraparticulate diffusion model plots for the adsorption of ARS on Ca-P

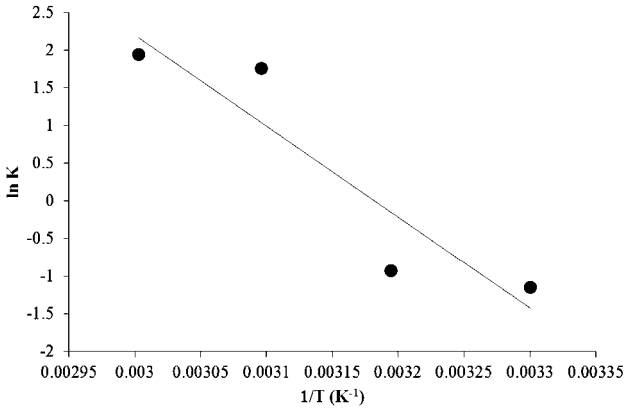

Fig. 11 Plot of ln K_d and $1/T$ for the for the adsorption of ARS on Ca-P

and the value of n (1.96) obtained in this study is an indication of favorable physical process and the normal Langmuir isotherm. For Redlich–Peterson isotherm parameters, Q_o values of 117.68 mg g^{-1} ($R^2 = 0.980$) is also close to the Langmuir maximum adsorption, 0.56 obtained the value of β show a favorable fit ($0 < \beta < 1$). Temkin isotherm constant b_T, which is related to the heat of adsorption obtained for this study is 102.76 ($R^2 = 0.991$) and its positive value indicates an endothermic process. The Dubinin–Radushkevich model and Sip isotherm parameters are also shown in Table 2. From the analysis of all the isotherms and the knowledge of the most their important parameters, the isotherms can be arranged according to their capacity to predict or their efficiency in predicting the experimental behavior of the ARS adsorption on Ca-P. With respect to Q_m (in descending order): Redlich–Peterson > Langmuir > Dubinin–Radushkevich > Sip. However, when R^2 is considered, the order is (in descending order): Sips > Dubinin–Radushkevich > Redlich–Peterson > Tempkin > Langmuir > Freundlich. The value of E obtained in D–R isotherm was found to be 1.32 kJ mol^{-1} and since $E < 8$ kJ mol^{-1}, it suggests that the adsorption mechanism is physical in nature (Helfferich 1962).

Adsorption kinetics

The plots of four different kinetic models used to explain the adsorption data are shown in Fig. 9. Pseudo-second-order kinetic models fit well with experimental data when compared with other models (Table 3). The rate constant from all the models showed an initial increase with increasing initial dye concentration, however, there is no significant increase as the concentration is increased up to 100 mg L^{-1}. This shows that at higher initial concentration the electrostatic interaction decreases at the site, thereby lowering the adsorption rate. The behavior of Elovich constant shows that the process of adsorption is more than one mechanism.

Adsorption mechanism

The mechanism of adsorption was investigated by subjecting the data to intraparticulate diffusion model. The plots are shown in Fig. 10. The linearity of the plot is not over the whole time range rather they exhibit multi-linearity revealing the existence of three successive

Table 4 Intraparticulate diffusion parameters

K_{1d} (mg g^{-1} $min^{-0.5}$)	1.60	3.64	5.09	6.50	9.28	9.25
C_1	0.67	1.64	1.94	2.48	3.21	3.87
R^2	0.969	0.965	0.975	0.973	0.978	0.969
K_{2d} (mg g^{-1} $min^{-0.5}$)	0.10	−0.02	−0.25	0.14	0.10	0.08
C_2	10.96	26.85	38.16	45.75	65.23	66.67
R^2	0.999	0.999	0.999	0.999	0.999	0.999
K_{3d} (mg g^{-1} $min^{-0.5}$)	0.09	0.02	0.28	0.03	0.08	−0.15
C_3	11.14	26.62	32.10	46.94	65.09	69.39
R^2	0.999	0.999	0.999	0.999	0.999	0.999

Table 5 Thermodynamic parameters for the adsorption of ARS on Ca-P

Temp (K)	ln K	ΔG (kJ mol^{-1})	ΔS (J mol^{-1})	ΔH (kJ mol^{-1})	R^2
303	−1.146	3.579	318.72	100.15	0.981
308	−0.919	0.391			
318	1.755	−2.795			
323	1.944	−5.982			

adsorption steps. The first stage is faster than the second, and it is attributed to the external surface adsorption referred to as the boundary layer diffusion. Thereafter, the second linear part is attributed to the intraparticle diffusion stage; this stage is the rate-controlling step. Table 3 shows the intraparticle model constants for the adsorption removal of ARS dye by Ca-P. The K_{di} values were found to be decreasing from first stage of adsorption toward the second stage. The increase in dye concentration results in an increase collision of dye molecules thereby affecting the dye diffusion rate.

Thermodynamic parameters

The free energy change, ΔG is obtained from Eqs. (20 and 21) according to the van't Hoff linear plots of ln K_d versus $1/T$ plot in Fig. 11. The thermodynamic parameters are presented in Table 4. From the Table, it is found that the negative value of ΔG as the temperature increases indicates the spontaneous nature of adsorption. Positive value of enthalpy change indicates that the adsorption process is endothermic in nature, and the negative value of change in internal energy (ΔG) show the spontaneous adsorption of ARS on to Ca-P. Positive values of entropy change show the increased randomness of the solution interface during the adsorption process (Table 5).

Conclusion

Calcium phosphate was prepared from $CaCO_3$ and HPO_5 and the physico-chemically characterized with XRD, SEM, and FTIR. Ca-P removed ARS from aqueous solution via adsorption process which depends on factors such as: adsorbent dosage, solution pH, temperature, initial dye concentration, and contact time. The percentage removal of the dye increased with pH up to 7, also contact time and current density increase influence the removal positively. Equilibrium data fitted very well with the isotherm equation in the order of Sips > Dubinin–Radushkevich > Redlich–Peterson > Tempkin > Langmuir > Freundlich. Langmuir adsorption isotherm confirmed the monolayer adsorption with capacity of 100.36 mg g^{-1} at 303 K. The kinetics of the process is best explained using a pseudo-second order kinetics model, with higher R^2 (Table 5). Intra-particle diffusion was not the sole rate-controlling factor. The thermodynamics parameters obtained indicate that the process is spontaneous endothermic nature of the process. In conclusion, Ca-P prepared from a cheap source has demonstrated the capability as a cheap adsorbent for remediation of dye-contaminated water.

Acknowledgments The financial support in the form of grants from CSIR, for 12 months TWAS-CSIR Postdoctoral Fellowship, FR Number: 3240275035, awarded to Abideen Idowu Adeogun that enables this work to be carried out. Also he is thankful to the authority of the Federal University of Agriculture, Abeokuta, Nigeria for granting the study leave to honor the fellowship.

References

Adeogun AI, Kareem SO, Durosanya JB, Balogun SE (2012) Kinetics and equilibrium parameters of biosorption and bioaccumulation of lead ions from aqueous solutions by *Trichoderma longi-brachiatum*. J Microbiol Biotechnol Food Sci 1:1221–1234

Ali M, Sreekrishnan TR (2001) Aquatic toxicity from pulp and paper mill effluents—a review. Adv Environ Res 5:175–196

Aniruldhan TS, Radhakrishnan PG (2008) Thermodynamics and kinetics of adsorption of Cu (II) from aqueous solutions onto a new cation exchanger derived from tamarind fruit shell. J Chem Thermodyn 40:702–709

Bello OS, Adeogun AI, Ajaelu JC, Fehintola EO (2008) Adsorption of methylene blue onto activated carbon derived from periwinkle shells: kinetics and equilibrium studies. Chem Ecol 24:285–295

Carneiro PA, Osugi ME, Fugivar CS, Boralle N, Furlan M, Zanoni MV (2005) Evaluation of different electrochemical methods on the oxidation and degradation of Reactive Blue 4 in aqueous solution. Chemosphere 59(3):431–439

Chien SH, Clayton WR (1980) Application of Elovich equation to the kinetics of phosphate release and sorption in soils. Soil Sci Soc Am J 44(2):265–268

Dubinin MM, Radushkevich LV (1947) Equation of the characteristic curve of activated charcoal, vol. 55. In: Proceedings of the academy of sciences, physical chemistry section, U.S.S.R., pp 331–333

El Boujaady H, Mourabet M, Bennani-Ziatni M, Taitai A (2014) Adsorption/desorption of Direct Yellow 28 on apatitic phosphate: mechanism, kinetic and thermodynamic studies. J Assoc Arab Univ Appl Sci 16:64–73

Freundlich HMF (1906) Over the adsorption in solution. J Phys Chem 57(1906):385–471

Helfferich F (1962) Ion-exchange. McGraw-Hill, New York

Kolpin DW, Furlong ET, Meyer MT, Thurman EM, Zaugg SD, Barber LB, Buxton HT (1999–2000) Pharmaceuticals, hormones and other organic wastewater contaminants in US streams: a national reconnaissance. Environ Sci Technol 36(6):1202–1211

Kundu S, Gupta AK (2006) Investigation on the adsorption efficiency of iron oxide coated cement (IOCC) towards As(V)—kinetics, equilibrium and thermodynamic studies. Colloid Surf A273:121–128

Langmuir I (1918) The adsorption of gases on plane surfaces of glass, mica and platinum. J Am Chem Soc 40:1361–1403

Lin GH, Brusick DJ (1992) Mutagenicity studies on two triphenylmethane dyes, bromophenol blue and tetrabromophenol blue. J Appl Toxicol 12(4):267–274

Lyubchik S, Lyubchik A, Fonseca I, Lygina O, Lyubchik S (2011) Comparison of the thermodynamic parameters estimation for the adsorption process of the metals from liquid phase on activated carbons. www.intechopen.com INTECH Open Access Publisher, 2011

Ma QY, Logan TJ, Traina SJ (1994) Effects of NO_3^-, Cl^-, F^-, SO_4^{2-}, and CO_3^{2-} on Pb^{2+} immobilization by hydroxyapatite. Environ Sci Technol 28:408–418

Malik PK (2004) Dye removal from wastewater using activated carbon developed from sawdust: adsorption equilibrium and kinetics. J Hazard Mater 113:81–88

Minh DP, Sebei H, Nzihou A, Sharrock P (2012) Apatitic calcium phosphates: synthesis, characterization and reactivity in the removal of lead(II) from aqueous solution. Chem Eng J 198–199:180–190

Minh DP, Tran ND, Nzihou A, Sharrock P (2014) Calcium phosphate based materials starting from calcium carbonate and orthophosphoric acid for the removal of lead(II) from an aqueous solution. Chem Eng J 243:280–288

Miyake M, Watanabe K, Nagayama Y, Nagasawa H, Suzuki T (1990) Synthetic carbonate apatites as inorganic cation exchangers. J Chem Soc Faraday Trans 86:2303–2306

Mobasherpour I, Salahi E, Pazouki M (2012) Comparative of the removal of Pb^{2+}, Cd^{2+} and Ni^{2+} by nano crystallite hydroxyapatite from aqueous solutions: adsorption isotherm study. Arab J Chem 5(4):439–446

Nzihou A, Sharrock P (2010) Role of phosphate in the remediation and reuse of heavy metal polluted wastes and sites. Waste Biomass Valoriz. 1:163–174

Panizza M, Michaud PA, Cerisola G, Comninellis C (2001) Electrochemical treatment of wastewaters containing organic pollutants on boron-doped diamond electrodes: prediction of specific energy consumption and required electrode area. Electrochem Commun 3:336–339

Rajgopalan S (1995) Water pollution problem in the textile industry and control. In: Trivedy RK (ed) Pollution management in industries. Environmental Publications, Karad, pp 21–44

Redlich O, Peterson DL (1959) A useful adsorption isotherm. J Phys Chem 63:1024–1026

Routh T (1998) Anaerobic treatment of vegetable tannery wastewater by UASB process Ind. J Environ Prot 20(2):115–123

Royer Betina, Cardoso Natali F, Lima Eder C, Ruiz Vanusa SO, Macedo Thaís R, Airoldi Claudio (2009) Organofunctionalized kenyaite for dye removal from aqueous solution. J Colloid Interface Sci 336(2):398–405

Shawabkeh RA, Tutunji MF (2003) Experimental study and modeling of basic dye sorption by diatomaceous clay. Appl Clay Sci 24(1–2):111–120

Sips R (1948) Combined form of Langmuir and Freundlich equations. J Chem Phys 16:490–495

Sun QY, Yang LZ (2003) The adsorption of basic dyes from aqueous solution on modified peat-resin particle. Water Res 37:1535–1544

Suzuki T, Ishigaki K, Miyake M (1984) Synthetic hydroxyapatites as inorganic cation exchangers, Part 3. Exchange characteristics of lead ions (Pb^{2+}). J Chem Soc Faraday Trans 1(80):3157–3165

Takagi O, Kuramoto N, Ozawa M, Suzuki S (2004) Adsorption/desorption of acidic and basic proteins on needle-like hydroxyapatite filter prepared by slip casting. Ceram Int 30:139–143

Tempkin MI, Pyzhev V (1940) Kinetics of ammonia synthesis on promoted iron catalyst. Acta Phys Chim USSR 12(1940):327–356

Weber WJ Jr, Morris JC (1963) Kinetics of adsorption on carbon from solution. J Sanit Eng Div-ASCE 89:31–59

Wei W, Wei Z, Zhao H, Li H, Hu F (2009) Elimination of the interference from nitrate ions on oxalic acid in RP-HPLC by solid-phase extraction with nanosized hydroxyapatite. J Liq Chromatogr Relat Technol 32:1–19

Wu FC, Tseng RL, Juang RS (2009) Initial behavior of intraparticle diffusion model used in the description of adsorption kinetics. Chem Eng J 153:1–8

Zucca P, Vinci C, Sollai F, Rescigno A, Sanjust E (2008) Degradation of Alizarin Red S under mild experimental conditions by immobilized 5,10,15,20-tetrakis(4-sulfonatophenyl) porphine–Mn(III) as a biomimetic peroxidase-like catalyst. J Mol Catal A: Chem 288:97–102